

1 **Differences in cofactor, oxygen and sulfur requirements influence niche adaptation in deep-**
2 **sea vesicomid clam symbioses**

3

4 Corinna Breusing^{1,*†}, Maëva Perez^{2,3†}, Roxanne A. Beinart¹, C. Robert Young²

5

6 ¹University of Rhode Island, Graduate School of Oceanography, Narragansett, RI, USA

7 ²National Oceanography Centre, Southampton, SO14 3ZH, UK

8 ³University of Montreal, Department of Biological Sciences, Montreal, Quebec H3T 1J4, Canada

9

10 *Corresponding author: corinnabreusing@gmail.com

11 †Authors contributed equally

12

13 Running title: Niche adaptation in clam symbionts

14

15 Keywords: Vesicomid clams, chemosynthetic endosymbionts, comparative genomics, vertical
16 transmission, reductive genome evolution, niche partitioning

17 **Abstract**

18 Vertical transmission of bacterial endosymbionts is accompanied by virtually irreversible gene
19 loss that can provide insights into adaptation to divergent ecological niches. While patterns of
20 genome reduction have been well described in some terrestrial symbioses, they are less
21 understood in marine systems where vertical transmission is relatively rare. The association
22 between deep-sea vesicomid clams and chemosynthetic Gammaproteobacteria is one example
23 of maternally inherited symbioses in the ocean. Differences in nitrogen and sulfur physiology
24 between the two dominant symbiont groups, *Ca. Ruthia* and *Ca. Vesicomysocius*, have been
25 hypothesized to influence niche exploitation, which likely affects gene content evolution in these
26 symbionts. However, genomic data are currently limited to confirm this assumption. In the
27 present study we sequenced and compared 11 vesicomid symbiont genomes with existing
28 assemblies for *Ca. Vesicomysocius okutanii* and *Ca. Ruthia magnifica*. Our analyses indicate
29 that the two vesicomid symbiont groups have a common core genome related to
30 chemosynthetic metabolism, but differ in their potential for nitrate respiration and flexibility to
31 environmental sulfide concentrations. Moreover, *Ca. Vesicomysocius* and *Ca. Ruthia* have
32 different enzymatic requirements for cobalamin and nickel and show contrasting capacities to
33 acquire foreign genetic material. Tests for site-specific positive selection in metabolic candidate
34 genes imply that the observed physiological differences are adaptive and thus likely correspond
35 to ecological niches available to each symbiont group. These findings highlight the role of niche
36 differentiation in creating divergent paths of reductive genome evolution in vertically transmitted
37 symbionts.

38 **Introduction**

39 Heritable symbioses with intracellular bacteria are observed across the eukaryotic domain of life
40 [1]. These symbioses can have significant impacts on the host's niche through their effects on
41 resource utilization, tolerance to stressors, and resistance to predators and pathogens [1–3].
42 Vertical transmission of bacterial lineages from parent to off-spring typically results in
43 irreversible genome degradation due to bottleneck effects, relaxed selective pressures and
44 restricted opportunities for horizontal gene transfer, limiting retention of genes to those that are
45 essential to the functioning of the host-symbiont association [3]. Thus, differences in gene
46 content among related symbionts can reveal how the host-symbiont pairs diverged in their niches
47 over evolutionary time. For example, divergence in plant host use between insect species is
48 evident in the biosynthetic pathways encoded in the genomes of their obligate endosymbionts
49 [4]. Ultimately, niche differentiation driven by differential gene loss has the potential to be an
50 important driver of host evolution through ecological speciation, as well as a significant factor in
51 the structure of host communities through its effects on competition and habitat partitioning
52 between host-symbiont pairs. Despite its importance for both ecological and evolutionary
53 processes, there is still a significant gap in our understanding of the patterns of gene/pathway
54 reduction in divergent vertically transmitted bacterial endosymbionts. This is especially true for
55 the heritable endosymbionts of marine organisms, since vertical transmission is less common
56 among aquatic symbioses [1].

57 Relatively strict vertical transmission of bacterial endosymbionts has been observed in
58 hydrothermal vent- and cold seep-associated deep-sea clams of the family Vesicomidae [5],
59 providing an opportunity to examine patterns of genome reduction in a marine symbiosis.
60 Vesicomid clams are nutritionally dependent on chemosynthetic maternally inherited

61 Gammaproteobacteria, which derive chemical energy from the oxidation of reduced sulfur
62 compounds to produce food for their hosts [6–10]. The clam-bacteria association is obligate,
63 given that vesicomid hosts have a highly reduced digestive system and cannot survive without
64 their symbionts [8]. Topological congruences between host mitochondrial and symbiont
65 phylogenetic trees suggest that symbionts co-evolve with their hosts [5], although disruptions of
66 these relationships have been reported due to infrequent horizontal transmission events that allow
67 for lateral gene transfer and homologous recombination between bacterial lineages [11–16].
68 Based on ribosomal sequence data, vesicomid symbionts are classified into two phylogenetic
69 clades [17]. Clade I symbionts (a.k.a *Ca. Vesicomiosocius*) are typically associated with hosts of
70 the *gigas*-group, including the nominal genera *Akebiconcha*, *Archivesica*, *Laubiericoncha* and
71 *Phreagena*, whereas clade II symbionts (a.k.a. *Ca. Ruthia*) associate with diverse groups of
72 vesicomid hosts [18]. Previous genomic comparisons between one representative symbiont
73 lineage from each clade (*Ca. Ruthia magnifica* and *Ca. Vesicomiosocius okutanii*) indicated that
74 the two groups differ in the amount of genome reduction [19–21]. This limited genomic data,
75 along with targeted PCR-based surveys, has suggested that *Ca. Vesicomiosocius* symbionts are
76 characterized by genomes with relatively low GC content that are deplete of critical genes for
77 nucleotide excision and recombination (e.g., *recA*, *mutY*, *uvrABCD*), indicating that they are in
78 an advanced stage of genome erosion. By contrast, *Ca. Ruthia* symbionts are thought to have
79 genomes with higher GC content that still contain intact homologs of these genes [17, 21, 22].

80 Variations in genome reduction and host affiliation between *Ca. Vesicomiosocius* and
81 *Ca. Ruthia* do not appear to be driven by adaptation to different broad-scale habitat types, as
82 clam species hosting lineages from both clades have been found at vents and seeps and often co-
83 occur at the same locality [8, 18, 23, 24]. However, the two symbiont clades appear to differ in

84 physiological characteristics related to nitrate reduction and sulfur metabolism, which may affect
85 microhabitat exploitation [8, 23], and could, thus, influence patterns of gene conservation
86 between clades. In fact, niche partitioning has been linked to patterns of gene loss and retention
87 in a variety of marine and freshwater bacteria [25, 26].

88 Genome sampling of multiple lineages within each symbiont clade is necessary to assess
89 whether the observed variation in nitrogen and sulfur physiology is a potential driver of niche
90 segregation between *Ca. Vesicomysocius* and *Ca. Ruthia*. To address this issue and identify
91 other metabolic differences between the two symbiont clades, we sequenced the genomes of 11
92 *Ca. Vesicomysocius* and *Ca. Ruthia* lineages and compared them with previous assemblies of
93 *Ca. V. okutanii* [20] and *Ca. R. magnifica* [19] (Table 1). Candidate metabolic genes that were
94 found to be differentially conserved between both symbiont clades were investigated for signals
95 of pervasive and episodic diversifying selection to assess their role in niche adaptation in these
96 symbionts.

97

98 **Results**

99 **GENOME ASSEMBLY METRICS**

100 Final assemblies for the eleven genomes comprised 1–39 contigs with a total size of 1.02–1.59
101 Mb, an N50 of 0.06–1.23 Mb, a GC content of 31.10–36.98%, and an average coverage of
102 49.20–153.10 (Table 1). Genomes of the different *Ca. Vesicomysocius* and *Ca. Ruthia* lineages
103 were comparable in size to those of *Ca. V. okutanii* and *Ca. R. magnifica*, respectively [19, 20],
104 and were assembled into single circular chromosomes, with two exceptions. Genomes of the
105 different *Ca. Ruthia* lineages were less homogeneous in size and typically larger than those of
106 the *Ca. Vesicomysocius* lineages. They also possessed higher gene density. The genome

107 assemblies of *Ca. R. phaseoliformis* and *Ca. R. southwardae* were the largest among all
108 symbiont genomes sequenced and were characterized by a relatively high amount of
109 fragmentation (Table 1).

110

111 **COMPARATIVE GENOMICS AND PHYLOGENOMICS**

112 Phylogenetic analyses of the *16S* rRNA gene and 739 orthologous single-copy gene clusters
113 identified the two previously described clades of vesicomylid symbionts [17], comprising the
114 nominal genera *Ca. Ruthia* and *Ca. Vesicomysocius* (Figure 1). While the topologies of the *Ca.*
115 *Vesicomysocius* lineages generally agreed between gene trees, the topologies of *Ca. R.*
116 *magnifica*, *Ca. R. pliocardia*, *Ca. R. phaseoliformis* and *Ca. R. southwardae* were incongruent
117 and poorly resolved based on the *16S* rRNA gene alone (Figure 1). Average nucleotide identities
118 (ANI) between lineages of the two clades were on average 82.93–83.85% in aligned nucleotide
119 regions, but only 42.49–66.97% if unaligned regions were considered (Table S1). ANIs within
120 clades were higher, with values of 93.55–99.99% (85.91–99.99%) between the different *Ca.*
121 *Vesicomysocius* lineages, and 87.80–95.22% (52.43–76.59%) between the different *Ca. Ruthia*
122 lineages (Table S1). Based on conservative species-level ANI cutoffs of 95–96% [47], these
123 values suggest that most symbiont lineages represent distinct bacterial species, except for *Ca. V.*
124 *diagonalis-extenta*, *Ca. V. okutanii-soyoe* and possibly *Ca. R. pacifica-rectimargo*.

125

126 **CORE GENOME CHARACTERISTICS**

127 All vesicomylid symbiont genomes shared 822 core gene clusters (consisting of 10,931 genes),
128 the majority of which were assigned to five broader functional categories: (1) energy production

129 and conversion, (2) amino acid metabolism and transport, (3) coenzyme metabolism and
130 transport, (4) translation, and (5) posttranslational modification (Figure 2; Table S2, S3).

131

132 *Energy metabolism*

133 The genomes of all *Ca. Ruthia* and *Ca. Vesicomysocius* lineages contained genes for the
134 oxidation of reduced sulfur compounds that serve as energy sources for chemoautotrophic
135 growth [9]. All genomes encoded the sulfur oxidation (SOX) multienzyme pathway (without
136 *soxCD*), the reversible dissimilatory sulfite reductase (rDSR) pathway as well as the adenosine
137 5'-phosphosulfate (APS) reductase pathway, indicating that these symbiont lineages are able to
138 oxidize sulfide, thiosulfate and/or sulfite for energy production (Table S2, S3) [48, 49]. In
139 addition, all genomes comprised genes for sulfide:quinone oxido-reductase type I and VI (SQR),
140 which can convert sulfide to sulfane sulfur [49]. With the exception of *Ca. V. soyoae 2* and *Ca.*
141 *V. okutanii*, the *Ca. Vesicomysocius* lineages contained two copies of the gene encoding SQR
142 type I, whereas this gene was present as a single copy in the *Ca. Ruthia* clade. In addition,
143 complex sulfur compounds may be made accessible via homologs of the polysulfide reductase
144 NrfD (Table S2, S3).

145 Based on their gene content, it is likely that all symbiont lineages can use a variety of
146 different enzymes to conserve energy via cross-membrane electron transport, including NADH-
147 ubiquinone oxidoreductase (Complex I), SQR, bacterial Rnf complex, cytochrome *bc₁* complex
148 (Complex III), terminal *cbb3*-type cytochrome-c-oxidase (Complex IV) and F₀F₁-type ATP
149 synthase (Complex V) (Table S2, S3).

150

151 *Inorganic carbon fixation and biosynthetic processes*

152 Members of the *Ca. Vesicomysocius* and *Ca. Ruthia* clades both encoded a form II ribulose
153 biphosphate carboxylase (cbbM) and other key enzymes for carbon assimilation via the Calvin-
154 Benson-Bassham cycle as well as a complete gene set for the non-oxidative branch of the
155 pentose phosphate pathway (Table S2, S3). Both symbiont clades lacked the gene for
156 sedoheptulose-bisphosphatase and might instead rely on a reversible pyrophosphate-dependent
157 phosphofructokinase (PPi-PFK) to interconvert between sedoheptulose 1,7-bisphosphate and
158 sedoheptulose 7-phosphate. PPi-PFK is likely also used to catalyze the phosphorylation of
159 fructose-6-phosphate to fructose 1,6-bisphosphate during glycolysis, as the gene for its ATP-
160 dependent homolog was absent in all vesicomysid symbiont genomes (Table S2, S3).

161 All symbiont lineages have the potential to further metabolize glycolytic intermediates
162 and end products via a partial tricarboxylic acid (TCA) cycle and pentose phosphate pathway to
163 produce precursors for the generation of several macronutrients, coenzymes and nucleotides
164 (Table S2, S3). While functional gene copies of α -ketoglutarate decarboxylase (E1 component of
165 the α -ketoglutarate dehydrogenase complex) and fumarate reductase Fe-S subunit appeared to be
166 missing or degenerated in all symbiont genomes, we found intact genes coding for malate
167 dehydrogenase. Both the *Ca. Ruthia* and *Ca. Vesicomysocius* genomes contained complete
168 gene sets for the independent biosynthesis of 19 amino acids and a variety of enzyme cofactors,
169 including most vitamins and their derivatives (e.g., coenzyme A, FAD, NAD⁺), hemes and
170 sirohemes, porphyrins, molybdopterin, ubiquinone and glutathione. The gene encoding
171 homoserine kinase (*thrB*), an essential enzyme in threonine biosynthesis, was missing from all
172 symbiont genomes, although it is possible that its function might be performed by a
173 serine/threonine kinase that was present in genomes from both the *Ca. Ruthia* and *Ca.*
174 *Vesicomysocius* clade. Similarly, a separate gene for histidinol phosphatase involved in

175 histidine biosynthesis was lacking from all symbiont genomes. However, the genomes of
176 symbionts from both clades contained homologs of the *hisB* gene, which encodes a bifunctional
177 imidazoleglycerol-phosphate dehydratase/histidinol-phosphatase. Pathways for the generation of
178 retinol, cobalamin, ascorbic acid, cholecalciferol, menaquinone and tocopherol were incomplete,
179 while protoheme biosynthesis appeared to occur through a novel form of protoporphyrinogen IX
180 oxidase (HemJ), which has so far mostly been described in cyanobacteria [50]. The *ubiD/ubiX*
181 gene complex for ubiquinone biosynthesis was absent in all symbiont lineages. The lack of
182 UbiD/UbiX might be compensated by UbiG via an alternative pathway that generates ubiquinone
183 through methylation of 3-polyprenyl-4,5-dihydroxybenzoate.

184

185 **CLADE- AND LINEAGE-SPECIFIC GENOME CHARACTERISTICS**

186 46 gene clusters (containing 321 genes) were specific to the *Ca. Ruthia* lineages, while six gene
187 clusters (containing 44 genes) occurred exclusively in the *Ca. Vesicomysocius* clade (Figure 1;
188 Tables S2, S3). In both clades, many of these gene clusters had unknown or poorly characterized
189 functions, whereas others implied clade-specific differences in cell wall biogenesis, translation
190 and post-translational modification (Figure 2; Tables S2, S3). Genomes in the *Candidatus Ruthia*
191 clade also contained a variety of gene clusters associated with biosynthetic and transport
192 processes that were absent in genomes from the *Ca. Vesicomysocius* clade (Figure 2; Tables
193 S2, S3). In several cases, genomes from the *Ca. Ruthia* and *Ca. Vesicomysocius* clades shared
194 the same gene clusters but differed in the amount of degeneration in the associated gene loci
195 (Table S3). An overview of the main differences between the two symbiont clades is given in
196 Figure 3.

197

198 *Methionine synthase*

199 *Candidatus* Ruthia and *Ca. Vesicomysocius* appear to use different enzymes for the synthesis
200 of methionine (Figure 3; Tables S2, S3). The gene for the cobalamin-dependent homocysteine
201 methyltransferase (*metH*) as well as genes for cobalamin (precursor) transport and conversion
202 (*btuM*, *btuR/cobA*) were conserved in genomes from the *Ca. Vesicomysocius* clade but were
203 missing or degenerated in all of the *Ca. Ruthia* lineages, except for *Ca. R. phaseoliformis* and
204 *Ca. R. southwardae*. Conversely, the gene for the cobalamin-independent version of this enzyme
205 (*metE*) along with its transcriptional activator (*metR*) were exclusively found in the *Ca. Ruthia*
206 symbiont genomes. Notably, almost all genes for *de novo* cobalamin biosynthesis were absent
207 from the investigated symbiont genomes, with the exception of cobyrinic acid A,C-diamide
208 synthase (*cbiA*), adenosylcobalamin/alpha-ribazole phosphatase (*cobC*) (all genomes) and the
209 high affinity cobalamin transporter BtuB (*Ca. V. gigas*).

210

211 *Nitrate reductase*

212 An operon coding for the membrane-bound nitrate-reductase complex NarGHIJ was conserved
213 in all *Ca. Vesicomysocius* symbiont genomes, but not in the *Ca. Ruthia* clade, which appeared
214 to contain non-functional remnants of this operon. Conversely, the symbionts of the *Ca. Ruthia*
215 clade encode the cytoplasmic assimilatory nitrate reductase NasA, which is degenerated in the
216 *Ca. Vesicomysocius* clade (Figure 3; Tables S2, S3).

217

218 *Cysteine dioxygenase and isocitrate lyase*

219 The gene coding for cysteine dioxygenase type I, which catalyzes the conversion of L-cysteine to
220 cysteine sulfinic acid, was conserved in all *Ca. Vesicomysocius* lineages, but absent or

221 degenerated in most *Ca. Ruthia* symbiont genomes (with the exception of *Ca. R. phaseoliformis*
222 and *Ca. R. pliocardia*). By contrast, only the *Ca. Ruthia* symbionts encode genes for isocitrate
223 lyase, a key enzyme of the glyoxylate cycle (Figure 3; Tables S2, S3).

224

225 *Transcription, translation and post-translational modification*

226 All vesicomylid symbiont genomes contained an operon for a Class Ia ribonucleotide reductase
227 (*nrdAB*), but only the *Ca. Ruthia* lineages appeared to also encode the gene for its transcriptional
228 repressor (*nrdR*). In addition, we found genes for several enzymes involved in protein
229 modification and response to cellular stress in the genomes of the *Ca. Ruthia* clade that were
230 absent in *Ca. Vesicomysocius* (Figure 3; Table S2, S3). For instance, all *Ca. Ruthia* lineages
231 contained genes for the GTP-binding protein HflX (exception: *Ca. R. pliocardia*), and the peptide
232 methionine sulfoxide reductase MsrB, which play a role in dissociation of translationally arrested
233 ribosomes [51], and protein repair after oxidative damage, respectively. Likewise, most *Ca.*
234 *Ruthia* lineages encoded genes for GidB and TrmL methyltransferases and a tRNA-
235 dihydrouridine synthase (Dus), which are involved in RNA modification, as well as a gene for
236 the ribosomal silencing factor RsfS, which is an important translational regulator.

237

238 *Cell wall and membrane biosynthesis*

239 *Ca. Ruthia* and *Ca. Vesicomysocius* differed in several genes that are involved in biogenesis of
240 the cellular envelope (Figure 3; Tables S2, S3). Although we found complete pathways for the
241 production of the common membrane lipid phosphatidylethanolamine in the genomes of all
242 vesicomylid symbiont lineages, genes for diacylglycerol kinase, which is necessary for
243 phospholipid recycling, was only present in the *Ca. Ruthia* clade. Similarly, all *Ca. Ruthia*

244 symbionts encoded a 1,6-anhydro-N-acetylmuramate kinase (AnmK) and an outer membrane
245 lipoprotein (SlyB), which are important for cell wall recycling and integrity, respectively. The
246 *Ca. Ruthia* lineages also contained a small-conductance mechanosensitive channel involved in
247 osmoregulation (MscS), a lipopolysaccharide (LPS) export system protein (LptA) involved in
248 LPS-translocation across the periplasm, and an N-acetyl-anhydromuramyl-L-alanine amidase
249 (AmpD) involved in cell wall degradation. Homologs of these genes were either completely
250 missing or pseudogenized in the *Ca. Vesicomysocius* symbionts. Both symbiont clades
251 possessed genes for peptidoglycan biosynthesis, although MurD, MurF, MraY and MurG
252 enzyme functionalities might be impaired or altered by the presence of internal stop codons in
253 the case of *Ca. V. diagonalis* and *Ca. V. extenta*. In addition, both symbiont clades contained
254 glycosyltransferases related to LPS biosynthesis, but appeared to encode different isoforms of
255 this enzyme.

256

257 *Transport across membrane*

258 Multiple components of a type I secretion system (lapC, lapB, lapE, and the secreted agglutinin
259 RTX) were found in all of the *Ca. Ruthia* symbionts except for *Ca. R. pliocardia*. By contrast,
260 this locus was missing in the *Ca. Vesicomysocius* clade (Figure 3; Table S3, S3). The *Ca.*
261 *Ruthia* symbionts also encoded a putative hydrogenase/urease accessory protein (HupE), which
262 is thought to be a nickel or cobalt transporter (Table S3) [52]. Although *hupE* is often associated
263 with operons coding for [NiFe] hydrogenases, we did not find genes encoding hydrogenase
264 subunits in any of the symbiont genomes. However, a gene encoding a nickel-dependent
265 glyoxalase I was present in the genomes of most *Ca. Ruthia* symbionts.

266

267 **GENE LOSS**

268 *DNA repair and recombination*

269 In agreement with Kuwahara et al. [17] and Shimamura et al. [22], genes of the nucleotide
270 excision repair pathway, *uvrA*, *uvrD*, *uvrD* paralog and *mfd*, were conserved in most symbiont
271 genomes, while *uvrB* and *uvrC* were degenerated in all *Ca. Vesicomysocius* lineages (Figure 3;
272 Table S2, S3). Within the *Ca. Ruthia* clade, *uvrA*, *uvrB*, *uvrD* paralog and *mfd* were present in all
273 lineages, whereas *uvrC* was lost in *Ca. R. pliocardia*, and *uvrD* was lost in *Ca. R. phaseoliformis*
274 and *Ca. R. southwardae*. Most *Ca. Ruthia* lineages contained genes for repair of alkylated DNA
275 (*alkD*) and strand breaks (*radA*; exception: *Ca. R. magnifica*), while homologs of these genes
276 were absent from all *Ca. Vesicomysocius* symbiont genomes. Furthermore, we found that
277 essential genes involved in SOS response to DNA damage, *recA*, *recFOR*, and *recX*, were lost in
278 the *Ca. Vesicomysocius* clade and *Ca. R. magnifica*. In the other *Ca. Ruthia* lineages, these
279 genes were conserved with the exception of *recF*, which was degenerated in *Ca. R. pacifica*, *Ca.*
280 *R. rectiomargo* and *Ca. R. pliocardia*, and *recO*, which was degenerated in *Ca. R.*
281 *phaseoliformis*. Likewise, the gene coding for RuvC, an essential component of the last step of
282 the *recF* and *recBCD* pathways for homologous recombination [53], as well as the genes coding
283 for the XerCD recombinase system and the DNA recombination protein RmuC were lost in the
284 *Ca. Vesicomysocius* clade, but conserved in most of the *Ca. Ruthia* lineages.

285

286 *Mobile elements and defense against pathogens*

287 The genomes of all vesicomysid symbionts are notably sparse in genes related to anti-viral
288 defense and transposition (Figure 3; Table S2, S3). Phage-related genes except for a putative
289 phage tape measure protein were completely missing in the *Ca. Vesicomysocius* clade, while a

290 few transposases (e.g., InsA, InsE, InsO, Tra8, RayT), integrases and other phage-derived
291 proteins were found in some of the *Ca. Ruthia* lineages, in particular *Ca. R. southwardae* and *Ca.*
292 *R. phaseoliformis*. All genomes contained genes coding for the lambda lysogenization regulator
293 HflD. In addition, remnants of type I restriction-modification systems (HsdMRS) and mRNA-
294 degrading toxin-antitoxin systems (e.g., MazEF) were present in the genomes of *Ca. R. pacifica*,
295 *Ca. R. rectimargo*, *Ca. R. phaseoliformis* and *Ca. R. southwardae*, but lost in all other symbiont
296 genomes. *Candidatus R. southwardae* and *Ca. R. phaseoliformis* further contained degenerated
297 operons for the 5-methylcytosine-specific restriction endonuclease McrBC. In addition,
298 putatively defunct versions of Cascade complex genes that were previously part of a
299 CRISPR/Cas system were found in *Ca. R. pliocardia* (*cas1*, *cas2*) and *Ca. R. southwardae* (*cas1*,
300 *cas3*).

301

302 **SITE-SPECIFIC POSITIVE SELECTION IN METABOLIC GENES**

303 Site-specific tests for adaptive evolution identified signals of positive selection in all 10
304 investigated candidate genes, except for *narI* (Table 3). Bayesian approximation analyses based
305 on FUBAR estimated that 1–2 sites were under pervasive diversifying selection in *cdo*, *hupE*,
306 *narG*, *nasA* and *sqrI* across the entire phylogeny. MEME analyses corresponded well with results
307 obtained by FUBAR, confirming sites under widespread positive selection and detecting 1–8
308 additional sites under episodic diversifying selection in a proportion of branches for all genes
309 (with the exception of *narI*) (Table 3). In three cases, p-values calculated by MEME were
310 insignificant for positively selected sites identified by FUBAR (*narG*: 451, *nasA*: 451, *sqrI*: 4).
311 However, since p-values were relatively close to the significance threshold of 0.1, it is possible
312 that statistical significance would have been observed with the inclusion of additional sequences.

313

314 **Discussion**

315 Given that obligate endosymbionts experience limited opportunities for acquisition of new genes
316 through horizontal transfer, differences in gene loss between symbiont lineages have the
317 potential to permanently separate holobiont niches, which has consequences for ecological
318 processes, like habitat use, and evolutionary processes, like host speciation. Differential gene
319 loss in divergent lineages of obligate, vertically transmitted endosymbionts has been well-
320 recognized to be important in the ecology and evolution of sap-feeding insects. For example,
321 differences in symbiont gene content may differentiate use of plant species by their insect hosts
322 [3, 4]. This symbiont-induced specialization on particular plant species has implications for the
323 evolutionary diversification of insect populations and species [3, 54]. However, outside the well-
324 studied insect-bacteria symbiosis [55–58], assessments of differential gene loss across clades and
325 lineages of vertically transmitted endosymbionts have been fairly limited, despite the broad
326 significance of gene loss patterns to our understanding of holobiont ecology and evolution.

327 As one of the few known examples of vertically transmitted marine symbioses, deep-sea
328 vesicomid clams represent an opportune system to study the process of incremental gene loss in
329 bacterial endosymbionts and its potential effect on niche differentiation in the ocean. In the
330 present study we compared the genomes of 13 lineages within the two dominant vesicomid
331 symbiont clades, *Ca. Ruthia* and *Ca. Vesicomysocius*, to assess commonalities and differences
332 in metabolic gene content and their eco-evolutionary implications. Similar to the vertically
333 transmitted endosymbionts of insects, which commonly display extreme stasis in a core genome
334 consistent with their primary role in nitrogen provisioning for their hosts [55–57], our analyses
335 reveal several shared features related to sulfur-based chemoautotrophic metabolism and energy

336 conversion (in line with [8]), which are fundamental to the nutritional services provided by the
337 endosymbionts of vesicomysid clams. By contrast, differences in gene loss among symbiont
338 lineages suggest a role for holobiont niche differentiation in shaping genome evolution. In the
339 endosymbionts of insects, differential gene loss is typically tied to variation in genes related to
340 components of the host diet, for example disparities in the availability of amino acids and
341 vitamins across food sources [3, 4, 58]. In the symbionts of vesicomysid clams, we observe
342 notable contrasts in cofactor, oxygen and sulfur requirements among clades. Several sites within
343 metabolic genes that were differentially conserved between *Ca. Ruthia* and *Ca.*
344 *Vesicomysocius* appeared to be at least episodically under diversifying selection, suggesting
345 that genetic differences between the two symbiont clades reflect adaptations to different
346 ecological niches.

347 For instance, *Ca. Ruthia* and *Ca. Vesicomysocius* encoded different, convergently
348 evolved types of methionine synthase [59], which vary in their dependence on vitamin B12 as
349 co-factor. While *Ca. Ruthia* contains the cobalamin-independent version MetE, *Ca.*
350 *Vesicomysocius* comprises homocysteine methyltransferase MetH, which is cobalamin-
351 dependent. As both clades appear unable to synthesize cobalamin *de novo* (like their eukaryotic
352 hosts), these findings indicate that the environmental availability of vitamin B12 has the potential
353 to be an important factor influencing the distribution of these taxa. Cobalamin independence in
354 *Ca. Ruthia* may offer an obvious selective advantage, by allowing these symbioses to exploit
355 niches that would otherwise be inaccessible. By contrast, the requirement for exogenous
356 vitamin B12 (or its derivatives) has the potential to limit the range of (micro)habitats *Ca.*
357 *Vesicomysocius*-based associations can colonize, unless cobalamin is acquired from a
358 (currently unknown) secondary symbiont, as for example seen in some insect-bacteria symbioses

359 [60]. Despite this potential cost, the retention of a cobalamin-dependent methionine synthase in
360 *Ca. Vesicomysocius* comes with an evolutionary benefit, given that MetH has a fifty fold
361 higher catalytic rate constant than MetE and thus enables faster growth [59]. The preservation of
362 cobalamin-dependent enzymes as a result of conferred physiological advantages appears to be
363 common across the eubacterial domain [61]. A recent genomic analysis by Shelton et al. [61]
364 showed that 86% of bacterial lineages have at least one cobalamin-dependent enzyme despite the
365 existence of a cobalamin-independent alternative, and that many of these lineages rely on
366 vitamin B12 production from other microbes in their environment. The importance of vitamin
367 B12 for the biology of the two symbiont groups is also evident in the fact that only *Ca. Ruthia*
368 encodes a transcriptional repressor (NrdR) for the ribonucleotide reductase NrdAB, a key
369 enzyme that controls the synthesis of DNA [62]. In *Ca. Vesicomysocius*, expression of NrdAB
370 is probably regulated by cobalamin, which has been shown to repress NrdAB transcription
371 through riboswitches [63].

372 There is evidence that *Ca. Vesicomysocius* and *Ca. Ruthia* differ in their requirements
373 for other enzyme cofactors, such as nickel. Only the *Ca. Ruthia* symbiont genomes encoded a
374 specific transporter for nickel uptake, and most of these lineages contained at least one
375 confirmed nickel-dependent enzyme, glyoxalase I [64]. By contrast, the ecological significance
376 of nickel for *Ca. Vesicomysocius* is questionable. Although an intact gene for a putative
377 Mg/Co/Ni transporter (MgtE) was present in the genomes of most vesicomysid symbionts,
378 electrophysiological analyses indicate that MgtE is not capable of transporting nickel [65]. In
379 addition, unambiguous annotations for nickel-dependent enzymes were missing from the
380 genomes of the *Ca. Vesicomysocius* symbionts. We found a gene encoding a protein of the

381 glyoxalase/bleomycin resistance protein/dioxygenase superfamily, but enzymes within this group
382 use a variety of different metals as cofactors and do not necessarily rely on nickel.

383 Apart from their contrasting dependencies on enzyme cofactors, *Ca. Ruthia* and *Ca.*
384 *Vesicomysocius* exhibit important differences in nitrogen metabolism [8]. While all *Ca.*
385 *Vesicomysocius* lineages encode genes for the membrane-bound dissimilatory nitrate reductase
386 NarGHIIJ, which utilizes nitrate as terminal electron acceptor for anaerobic respiration, the *Ca.*
387 *Ruthia* symbionts contain genes for the assimilatory nitrate reductase NasA, which metabolizes
388 nitrate as nitrogen source for growth [66]. Despite the distinct physiological functions of these
389 enzymes, ammonium generated through dissimilatory nitrate reduction is likely also used for
390 biosynthetic purposes in *Ca. Vesicomysocius* given the absence of an assimilatory equivalent.
391 As noted by Newton et al. [8], the use of NarGHIIJ for nitrate reduction in *Ca. Vesicomysocius*
392 might allow these symbioses to inhabit hypoxic environments, since the use of nitrate as an
393 electron acceptor would reduce the symbiont's requirement for oxygen and, consequently, also
394 reduce the oxygen requirement for the total holobiont. Segregation into differentially oxygenated
395 niches might further explain why several genes involved in oxidative stress response (e.g., *uvrA*,
396 *recA*, *dsbC*, *msrB*) were largely conserved in *Ca. Ruthia* but not in *Ca. Vesicomysocius*.

397 The presence of a single (or predominant) metabolic pathway for methionine biosynthesis
398 and nitrate reduction in each symbiont group suggests a clearing of redundancies through
399 reductive genome evolution, but the differential loss between the groups does not appear to be
400 random. Indeed, we observe very different patterns of *narGHIIJ* and *metH* pseudogenization even
401 between very closely related symbionts (e.g., *Ca. R. pacifica* and *Ca. R. rectimargo*), suggesting
402 that the inactivation of these genes has happened multiple times throughout the recent history of
403 the *Ca. Ruthia* clade. Elimination of functionally redundant genes is also apparent in the low

404 level of duplication in the genomes of all vesicomysid symbionts. Interestingly, almost all *Ca.*
405 *Vesicomysocius* lineages, but none of the *Ca. Ruthia* symbionts contain two copies of SQR
406 type I. Previous studies have shown that SQRs have different substrate concentration optima,
407 with SQR type I being adapted to low sulfide concentrations in the micromolar range, and SQR
408 type VI being adapted to elevated sulfide concentrations in the millimolar range [67–69].
409 Perhaps the two SQR type I versions in *Ca. Vesicomysocius* are necessary to maximize sulfide
410 oxidation at different micromolar H₂S concentrations, thereby optimizing the holobionts'
411 adaptability to fluctuations in environmental reductant levels. Variations in host and symbiont
412 metabolic plasticity and enzyme properties in relation to sulfur availability or processing might
413 further be important for avoiding competition between sympatric species [23, 24]. For example,
414 Goffredi and Barry [23] suggested that adaptation to different sulfide levels plays a role in niche
415 partitioning of co-occurring clam species in Monterey Bay. *Ca. Vesicomysocius*-based
416 associations have been found to occupy microhabitats with higher levels of sulfide, while *Ca.*
417 *Ruthia*-based symbioses inhabit zones with lower concentrations of this reductant [23].
418 Hydrogen sulfide can disrupt aerobic respiration and must be neutralized to avoid toxic effects
419 on the animal host. In a variety of symbiont-bearing vent and seep invertebrates, the non-
420 proteinogenic amino acid thiotaurine, a derivative of hypotaurine, has been shown to play a role
421 in sulfide detoxification [70–72]. Our analyses imply that in *Ca. Vesicomysocius*-based
422 associations host H₂S tolerance might be amplified (or solely mediated) by symbiont-derived
423 thiotaurine, given that all lineages of the *Ca. Vesicomysocius* clade encode genes for cysteine
424 dioxygenase, a key enzyme in taurine/hypotaurine biosynthesis. If *Ca. Vesicomysocius*-based
425 symbioses are typically exposed to higher concentrations of sulfide, symbiont-driven sulfide
426 inactivation might be another adaptation to the specific ecological niches of these taxa.

427 The role of cysteine dioxygenase in bacteria is relatively poorly understood, although a
428 few functions have been suggested [73]. For example, its activity is likely relevant for
429 replenishing the internal sulfur and carbon pools, since its product cysteine sulfinic acid can be
430 transaminated to generate sulfite and pyruvate [73]. We suggest another potential physiological
431 role for this enzyme that might help to illuminate how *Ca. Vesicomysocius* replenishes
432 metabolic intermediates of its partial TCA cycle, in particular succinate. While succinate
433 regeneration via the glyoxylate shunt has been proposed for *Ca. Ruthia*, the mechanism of
434 succinate recycling in *Ca. Vesicomysocius* has so far remained unclear. Newton et al. [8]
435 hypothesized that succinate might be taken up from the host's cytoplasm via a putative sugar
436 transporter. Although we did find a gene for a potential di- and tricarboxylate transporter
437 (COG0471) in the genomes of all *Ca. Vesicomysocius* lineages, it is also possible that succinate
438 might be restored through anaplerotic reactions resulting from the degradation of cysteine.
439 Cysteine is metabolized by cysteine dioxygenase to produce cysteine sulfinic acid, which
440 spontaneously oxidizes to L-cysteate. L-cysteate could be further decarboxylated to taurine via
441 glutamate decarboxylase and subsequently converted via taurine dioxygenase to yield sulfite,
442 succinate, CO₂ and aminoacetaldehyde. It is currently unknown whether this pathway occurs in
443 *Ca. Vesicomysocius*, but it represents a viable hypothesis for a host-independent regeneration
444 of succinate.

445 In agreement with Kuwahara et al. [21], our analyses indicate that *Ca. Ruthia* and *Ca.*
446 *Vesicomysocius* differ in several enzymes that affect the structure and composition of the
447 bacterial cell wall and membrane. In particular, symbionts of the *Ca. Ruthia* clade contained a
448 variety of exclusive genes involved in cell envelope biosynthesis, which may correspond to
449 clade- or species-specific responses to pathogens and/or interactions with their clam hosts.

450 Compared to *Ca. Vesicomysocius*, multiple lineages of the *Ca. Ruthia* group retain remnants of
451 genes involved in anti-viral defense and transposition, possibly due to increased selective
452 pressures or higher frequency of homologous recombination resulting from leaky vertical
453 transmission. Previous studies suggested that occasional horizontal transmission is present in
454 various vesicomysid symbiont species [11, 12, 15] and seems to be mostly a result of host-to-host
455 transfer [13, 14] or inter-specific hybridization [16]. Occasional horizontal acquisition creates
456 opportunities for recombination between symbiont lineages that decelerates the increasing
457 genome reduction and the ultimate evolutionary enslavement of these endosymbionts by their
458 hosts [9]. *Candidatus R. southwardae* and *Ca. R. phaseoliformis* exhibited the lowest degree of
459 genome erosion among all vesicomysid symbionts analyzed, which could imply that gene
460 salvaging through homologous recombination is particularly frequent in these lineages. *Ca. R.*
461 *southwardae* and *Ca. R. phaseoliformis* are associated with two *Abyssogena* species, which
462 exclusively occur at abyssal depths and belong to a more recently radiated group of vesicomysid
463 host taxa [18] where symbiont switching events have been observed [11, 15]. Thus, it is possible
464 that depth-related environmental stressors might select for gene retention, while a proclivity to
465 acquire foreign symbionts might favor recombination, thereby decreasing the rate of genome
466 reduction in these symbiont lineages. Increased taxonomic and population level sampling could
467 help to clarify the evolutionary processes and rates involved in gene content evolution in these
468 taxa.

469 The differential patterns of gene loss between *Ca. Vesicomysocius* and *Ca. Ruthia*
470 reiterate that reductive genome evolution does not follow a universal trajectory but is a reflection
471 of the ecological and evolutionary context of the respective host-symbiont association [25, 26].
472 Convergent gene loss and pseudogenization imply common evolutionary pressures for some

473 genes, whereas selection on codons and lineage-specific gene retention imply niche-specific
474 adaptation in others. In both symbiont clades, physiological differences related to nickel,
475 cobalamin, oxygen and sulfur requirements appear to mediate microhabitat segregation and the
476 generation of divergent niche-specific gene pools. Future studies linking environmental data with
477 symbiont genomic information will be helpful to obtain further insights into the ecological basis
478 of reductive genome evolution in the symbionts of deep-sea vesicomysid clams.

479

480 **Materials and Methods**

481 **SAMPLE COLLECTION AND DNA EXTRACTION**

482 Clam specimens were collected from nine cold seep and hydrothermal vent sites in the Pacific
483 and Atlantic Ocean during research expeditions between 1994 and 2004 (Table 2). Upon
484 recovery of the submersibles, samples were dissected and frozen at -80°C . DNA was extracted
485 onshore from symbiont-bearing gill tissues with the DNeasy Blood & Tissue kit (Qiagen, Hilden,
486 Germany) following manufacturer's instructions. Clam host species were identified via
487 mitochondrial cytochrome-c-oxidase I (*COI*) sequencing using vesicomysid-specific primers [27].
488 For the remainder of this manuscript we will use the previously erected symbiont genus names
489 *Ca. Vesicomysocius* and *Ca. Ruthia* plus the host species name to define the different symbiont
490 lineages.

491

492 **METAGENOMIC SEQUENCING, ASSEMBLY AND ANNOTATION**

493 Barcoded 2x300 bp metagenomic libraries were prepared with the KAPA Hyperplus Library
494 Preparation kit (KAPA Biosystems, Wilmington, MA, US) and sequenced on an Illumina MiSeq
495 system at the National Oceanography Centre (Southampton, UK). After initial quality checks

496 with FASTQC v0.11.5 [28], reads were adapter-clipped with TRIMMOMATIC v0.36 [29] and
497 assembled *de novo* with VELVET v1.2.10 [30], SPADES v3.13.1 [31] or GENEIOUS v10.1.3
498 (<http://www.geneious.com/>) using manual optimizations of k-mer size distribution and read
499 depth. Symbiont contigs were binned based on GC content and read coverage profiles and
500 subsequently scaffolded with SSPACE v2.0 [32]. For assemblies that resulted in a single scaffold,
501 we tried to circularize the genomes by reassembling and overlapping the last 5000 bp of each
502 contig end with SPADES. The final symbiont genome assemblies were annotated with RAST v2.0
503 [33] and investigated for quality with QUAST v5.0.0 [34]. Positional homologs between
504 assemblies were identified by aligning the symbiont genomes with PROGRESSIVEMAUVE
505 v20150213 [35], using a minimum identity cutoff of 30% and a minimum coverage cutoff of
506 60%.

507

508 **COMPARATIVE GENOMICS**

509 We ran the ANVI'0 v6.2 pangenomics workflow [36, 37] to assess core and lineage-specific
510 features of the *Ca. Vesicomysocius* and *Ca. Ruthia* genomes and to determine phylogenomic
511 relationships based on 739 single copy gene clusters. We used the "--ncbi-blast" option to
512 calculate amino acid sequence similarities and the MCL algorithm to define protein clusters
513 based on the following settings: minbit = 0.5, mcl-inflation = 6, min-occurrence = 1. Gene
514 cluster annotations were based on the Cluster of Orthologous Groups (COG) database [38].
515 Complementarily, phylogenetic analyses of the symbiont *16S* rRNA gene were performed with
516 MRBAYES v3.2.7a [39] in CIPRES v3.3 [40] based on a GTR+I+G substitution model. Prior to
517 phylogenetic reconstruction, all sequences were aligned against the global SILVA *16S* rRNA
518 alignment with SINA v1.2.11 [41] to account for secondary structure of the *16S* rRNA. We ran

519 three heated chains and one cold chain for 1,100,000 generations, sampling every 100
520 generations and discarding the first 100,000 generations as burn-in. The symbiont *16S* rRNA
521 gene sequence of the *Bathymodiolus thermophilus* symbiont (CP024634) was used as outgroup
522 for tree rooting. MCMC convergence was assessed with TRACER v1.7.1 [42].

523

524 TESTS FOR ADAPTIVE EVOLUTION

525 Our comparative genomic analyses identified a number of differentially conserved candidate
526 genes that might affect niche adaptation in *Ca. Ruthia* and *Ca. Vesicomysocius*: cysteine
527 dioxygenase (*cdo*), hydrogenase/urease accessory protein (*hupE*), methionine synthase (*metE*,
528 *metH*), respiratory nitrate reductase (*narGHIIJ*), assimilatory nitrate reductase (*nasA*), and
529 sulfide:quinone oxidoreductase type I (*sqrI*). To examine whether sites within these genes are
530 subject to pervasive or episodic diversifying selection we applied Bayesian approximation and
531 mixed-effects maximum likelihood approaches implemented in FUBAR v2.2 [43] and MEME
532 v2.1.1.2 [44], respectively. Both programs infer per-site nonsynonymous (dN) and synonymous
533 (dS) substitution rates for a given coding nucleotide alignment and matching phylogenetic tree,
534 but aim to detect different forms of positive selection. FUBAR determines sites that show signals
535 of pervasive positive selection across the entire phylogeny [43], while MEME identifies sites that
536 are evolving under episodic positive selection in a proportion of branches [44]. Analyses were
537 performed using all available symbiont sequences for a gene, including positional homologs of
538 the phylogenetically related *Bathymodiolus thermophilus* symbiont (CP024634), to increase
539 statistical power. Input trees for model optimization were generated with FASTTREE v2.1.11 [45]
540 under a GTR substitution model. FUBAR analyses included 5 MCMC chains, with chain lengths
541 of 2000000, a burn-in of 1000000 and a sample size of 100, while MEME analyses were run with

542 default settings. Because site-level tests for positive selection are relatively conservative, we
543 chose recommended p-value thresholds of 0.1 for MEME and posterior probability thresholds of
544 0.9 for FUBAR to assess statistical significance [46].

545

546 DATA AVAILABILITY

547 The final genome assemblies including raw Illumina data have been uploaded to GenBank and
548 the Sequence Read Archive under BioProject number PRJNA641445. Host mitochondrial *COI*
549 sequences have been deposited in GenBank under accession numbers MT894120–MT894130.

550

551 References

- 552 1. Russell SL. Transmission mode is associated with environment type and taxa across bacteria-
553 eukaryote symbioses: a systematic review and meta-analysis. *FEMS Microbiol Lett.* 2019;
554 366(3): fnz013.
- 555 2. Fisher RM, Henry LM, Cornwallis CK, Kiers ET, West SA. The evolution of host-symbiont
556 dependence. *Nat Commun.* 2017; 8: 15973.
- 557 3. Bennett GM, Moran NA. Heritable symbiosis: The advantages and perils of an evolutionary
558 rabbit hole. *PNAS* 2015; 112(33): 10169–10176.
- 559 4. Hansen AK, Moran NA. The impact of microbial symbionts on host plant utilization by
560 herbivorous insects. *Mol Ecol.* 2014; 23: 1473–1496.
- 561 5. Peek AS, Feldman RA, Lutz RA, Vrijenhoek RC. Cospeciation of chemoautotrophic bacteria
562 and deep-sea clams. *PNAS* 1998; 95(17): 9962–9966.
- 563 6. Childress JJ, Fisher CR, Favuzzi JA, Sanders NK. Sulfide and carbon dioxide uptake by the
564 hydrothermal vent clam, *Calyptogena magnifica*, and its chemoautotrophic symbionts.
565 *Physiol. Zool.* 1991; 64: 1444–1470.
- 566 7. Robinson JJ, Cavanaugh CM. Expression of form I and form II Rubisco in chemoautotrophic
567 symbioses: Implications for the interpretation of stable carbon isotope values. *Limnol*
568 *Oceanogr.* 1995; 40: 1496–1502.
- 569 8. Newton IL, Girguis PR, Cavanaugh CM. Comparative genomics of vesicomid clam
570 (*Bivalvia*: Mollusca) chemosynthetic symbionts. *BMC Genomics* 2008; 9: 585.
- 571 9. Vrijenhoek RC. Genetics and evolution of deep-sea chemosynthetic bacteria and their
572 invertebrate hosts. In: Kiel S (ed). *The Vent and Seep Biota*. (Springer, Dordrecht,
573 Netherlands, 2010) pp 15–49.
- 574 10. Dubilier N, Bergin C, Lott C. Symbiotic diversity in marine animals: the art of harnessing
575 chemosynthesis. *Nat Rev Microbiol.* 2008; 6: 725–740.
- 576 11. Stewart FJ, Young CR, Cavanaugh CM. Lateral symbiont acquisition in a maternally
577 transmitted chemosynthetic clam endosymbiosis. *Mol Biol Evol.* 2008; 25: 673–687.

- 578 12. Stewart FJ, Young CR, Cavanaugh CM. Evidence for homologous recombination in
579 intracellular chemosynthetic clam symbionts. *Mol Biol Evol.* 2009; 26: 1391–1404.
- 580 13. Decker C, Olu K, Arnaud-Haond S, Duperron S. Physical proximity may promote lateral
581 acquisition of bacterial symbionts in vesicomid clams. *PLoS ONE* 2013; 8: e64830.
- 582 14. Ikuta T, Igawa K, Tame A, Kuroiwa T, Kuroiwa H, *et al.* Surfing the vegetal pole in a small
583 population: extracellular vertical transmission of an 'intracellular' deep-sea clam symbiont. *R*
584 *Soc Open Sci.* 2016; 3: 160130.
- 585 15. Ozawa G, Shimamura S, Takaki Y, Takishita, Ikuta T, *et al.* Ancient occasional host
586 switching of maternally transmitted bacterial symbionts of chemosynthetic vesicomid
587 clams. *Genome Biol Evol.* 2017; 9: 2226–2236.
- 588 16. Breusing C, Johnson SB, Vrijenhoek RC, Young CR. Host hybridization as a potential
589 mechanism of lateral symbiont transfer in deep-sea vesicomid clams. *Mol Ecol.* 2019; 28:
590 4697–4708.
- 591 17. Kuwahara H, Takaki Y, Shimamura S, Yoshida T, Maeda T, *et al.* Loss of genes for DNA
592 recombination and repair in the reductive genome evolution of thioautotrophic symbionts of
593 *Calyptogena* clams. *BMC Evol Biol.* 2011; 11: 285.
- 594 18. Johnson SB, Krylova EM, Audzijonyte A, Sahling H, Vrijenhoek RC. Phylogeny and origins
595 of chemosynthetic vesicomid clams. *Syst Biodivers.* 2017; 15(4): 346–360.
- 596 19. Newton IL, Woyke T, Auchtung TA, Dilly GF, Dutton RJ, *et al.* The *Calyptogena magnifica*
597 chemoautotrophic symbiont genome. *Science* 2007; 315: 998–1000.
- 598 20. Kuwahara H, Yoshida T, Takaki Y, Shimamura S, Nishi S, *et al.* Reduced genome of the
599 thioautotrophic intracellular symbiont in a deep-sea clam, *Calyptogena okutanii*. *Curr. Biol.*
600 2007; 17: 881–886.
- 601 21. Kuwahara H, Takaki Y, Yoshida T, Shimamura S, Takishita K, *et al.* Reductive genome
602 evolution in chemoautotrophic intracellular symbionts of deep-sea *Calyptogena* clams.
603 *Extremophiles* 2008; 12: 365–374.
- 604 22. Shimamura S, Kaneko T, Ozawa G, Matsumoto MN, Koshiishi T, *et al.* Loss of genes related
605 to Nucleotide Excision Repair (NER) and implications for reductive genome evolution in
606 symbionts of deep-sea vesicomid clams. *PLoS ONE* 2017; 12: e0171274.
- 607 23. Goffredi SK, Barry JP. Species-specific variation in sulfide physiology between closely
608 related Vesicomid clams. *Mar Ecol Prog Ser.* 2002; 225: 227–238.
- 609 24. Cruaud P, Decker C, Olu K, Arnaud-Haond S, Papat C, *et al.* Ecophysiological differences
610 between vesicomid species and metabolic capabilities of their symbionts influence
611 distribution patterns of the deep-sea clams. *Mar Ecol.* 2019; 40: e12541.
- 612 25. Luo H, Huang Y, Stepanauskas R, Tang J. Excess of non-conservative amino acid changes in
613 marine bacterioplankton lineages with reduced genomes. *Nat Microbiol.* 2017; 2: 17091.
- 614 26. Baumgartner M, Roffler S, Wicker T, Pernthaler J. Letting go: bacterial genome reduction
615 solves the dilemma of adapting to predation mortality in a substrate-restricted
616 environment. *ISME J.* 2017; 11(10): 2258–2266.
- 617 27. Peek A, Gustafson R, Lutz R, Vrijenhoek R. Evolutionary relationships of deep-sea
618 hydrothermal vent and cold-water seep clams (Bivalvia: Vesicomidae): Results from the
619 mitochondrial cytochrome oxidase subunit I. *Mar Biol.* 1997; 130: 151–161.
- 620 28. Andrews S. FastQC: a quality control tool for high throughput sequence data. 2010
621 <http://www.bioinformatics.babraham.ac.uk/projects/fastqc/>
- 622 29. Bolger AM, Lohse M, Usadel B. Trimmomatic: a flexible trimmer for Illumina sequence
623 data. *Bioinformatics* 2014; 30: 2114–2120.

- 624 30. Zerbino DR, Birney E. Velvet: algorithms for de novo short read assembly using de Bruijn
625 graphs. *Genome Res.* 2008; 18: 821–829.
- 626 31. Bankevich A, Nurk S, Antipov D, Gurevich AA, Dvorkin M, *et al.* SPAdes: a new genome
627 assembly algorithm and its applications to single-cell sequencing. *J Comput Biol.* 2012;
628 19(5): 455–477.
- 629 32. Boetzer M, Henkel CV, Jansen HJ, Butler D, Pirovano W. Scaffolding pre-assembled contigs
630 using SSPACE. *Bioinformatics* 2010; 27(4): 578–579.
- 631 33. Aziz RK, Bartels D, Best AA, DeJongh M, Disz T, *et al.* The RAST Server: rapid
632 annotations using subsystems technology. *BMC Genomics* 2008; 9: 75.
- 633 34. Gurevich A, Saveliev V, Vyahhi N, Tesler G. QUAST: quality assessment tool for genome
634 assemblies. *Bioinformatics* 2013; 29: 1072–1075.
- 635 35. Darling AE, Mau B, Perna NT. progressiveMauve: multiple genome alignment with gene
636 gain, loss and rearrangement. *PLoS ONE* 2010; 5: e11147.
- 637 36. Eren AM, Esen ÖC, Quince C, Vineis JH, Morrison HG, *et al.* Anvi'o: an advanced analysis
638 and visualization platform for 'omics data. *PeerJ* 2015; 3: e1319.
- 639 37. Delmont TO, Eren AM. Linking pangenomes and metagenomes: the *Prochlorococcus*
640 metapangenome. *PeerJ* 2018; 6: e4320.
- 641 38. Tatusov RL, Galperin MY, Natale DA, Koonin EV. The COG database: a tool for genome-
642 scale analysis of protein functions and evolution. *Nucleic Acids Res.* 2000; 28(1): 33–36.
- 643 39. Huelsenbeck JP, Ronquist F. MrBAYES: Bayesian inference of phylogenetic trees.
644 *Bioinformatics* 2001; 17: 754–755.
- 645 40. Miller MA, Pfeiffer W, Schwartz T. Creating the CIPRES Science Gateway for inference of
646 large phylogenetic trees. In: *Proceedings of the Gateway Computing Environments*
647 *Workshop (GCE)*. (New Orleans, LA, USA, 2010) pp 1–8.
- 648 41. Pruesse E, Peplies J, Glöckner FO. SINA: accurate high-throughput multiple sequence
649 alignment of ribosomal RNA genes. *Bioinformatics* 2012; 28: 1823–1829.
- 650 42. Rambaut A, Drummond AJ, Xie D, Baele G, Suchard MA. Posterior summarization in
651 Bayesian phylogenetics using Tracer 1.7. *Syst Biol.* 2018; 67(5): 901.
- 652 43. Murrell B, Moola S, Mabona A, Weighill T, Sheward D, *et al.* FUBAR: A Fast,
653 Unconstrained Bayesian AppRoximation for inferring selection. *Mol Biol Evol.* 2013; 30(5):
654 1196–1205.
- 655 44. Murrell B, Wertheim JO, Moola S, Weighill T, Scheffler K, *et al.* Detecting individual sites
656 subject to episodic diversifying selection. *PLoS Genet.* 2012; 8: e1002764.
- 657 45. Price MN, Dehal PS, Arkin AP. FastTree 2 – Approximately maximum-likelihood trees for
658 large alignments. *PLoS ONE* 2010; 5(3): e9490.
- 659 46. Spielman SJ, Weaver S, Shank SD, Magalis BR, Li M, *et al.* Evolution of viral genomes:
660 Interplay between selection, recombination, and other forces. In: Anisimova M (ed).
661 *Evolutionary Genomics. Methods in Molecular Biology.* (Humana, New York, NY, 2019) pp
662 427–468.
- 663 47. Richter M, Rosselló-Móra R. Shifting the genomic gold standard for the prokaryotic species
664 definition. *PNAS* 2009; 106: 19126–19131.
- 665 48. Nakagawa S, Takai K. Deep-sea vent chemoautotrophs: diversity, biochemistry and
666 ecological significance. *FEMS Microbiol Ecol.* 2008; 65: 1–14.
- 667 49. Klatt JM, Polerecky L. Assessment of the stoichiometry and efficiency of CO₂ fixation
668 coupled to reduced sulfur oxidation. *Front Microbiol.* 2015; 6: 484.

- 669 50. Kato K, Tanaka R, Sano S, Tanaka A, Hosaka H. Identification of a gene essential for
670 protoporphyrinogen IX oxidase activity in the cyanobacterium *Synechocystis* sp. PCC6803.
671 PNAS 2010; 107(38): 16649–16654.
- 672 51. Zhang Y, Mandava CS, Cao W, Li X, Zhang D, *et al.* HflX is a ribosome-splitting factor
673 rescuing stalled ribosomes under stress conditions. Nat Struct Mol Biol. 2015; 22(11): 906–
674 913.
- 675 52. Eitinger T, Suhr J, Moore L, Smith JAC. Secondary transporters for nickel and cobalt ions:
676 theme and variations. Biometals 2005; 18(4): 399–405.
- 677 53. Connolly B, Parsons CA, Benson FE, Dunderdale HJ, Sharples GJ, *et al.* Resolution of
678 Holliday junctions in vitro requires the *Escherichia coli* *ruvC* gene product. PNAS 1991;
679 88(14): 6063–6067.
- 680 54. Janson EM, Stireman III JO, Singer MS, Abbot P. Phytophagous insect–microbe mutualisms
681 and adaptive evolutionary diversification. Evolution 2008; 62(5): 997–1012.
- 682 55. Patiño-Navarrete R, Moya A, Latorre A, Peretó J. Comparative Genomics of *Blattabacterium*
683 *cuenoti*: The frozen legacy of an ancient endosymbiont genome. Genome Biol Evol. 2013;
684 5(2): 351–361.
- 685 56. Manzano-Marín A, Coeur d’acier A, Clamens A, Orvain C, Cruaud C, *et al.* Serial horizontal
686 transfer of vitamin-biosynthetic genes enables the establishment of new nutritional symbionts
687 in aphids’ di-symbiotic systems. ISME J. 2020; 14: 259–273.
- 688 57. Chong R, Park H, Moran NA. Genome evolution of the obligate endosymbiont *Buchnera*
689 *aphidicola*. Mol Biol Evol. 2019; 36(7): 1481–1489.
- 690 58. Williams LE, Wernegreen JJ. Genome evolution in an ancient bacteria-ant symbiosis:
691 parallel gene loss among *Blochmannia* spanning the origin of the ant tribe Camponotini.
692 PeerJ 2015; 3: e881.
- 693 59. González JC, Banerjee RV, Huang S, Sumner JS, Matthews RG. Comparison of cobalamin-
694 independent and cobalamin-dependent methionine synthases from *Escherichia coli*: two
695 solutions to the same chemical problem. Biochemistry 1992; 31(26): 6045–6056.
- 696 60. McCutcheon JP, McDonald BR, Moran NA. Convergent evolution of metabolic roles in
697 bacterial co-symbionts of insects. PNAS 2009; 106(36): 15394–15399.
- 698 61. Shelton AN, Seth EC, Mok KC, Han AW, Jackson SN, *et al.* Uneven distribution of
699 cobamide biosynthesis and dependence in bacteria predicted by comparative genomics.
700 ISME J. 2019; 13: 789–804.
- 701 62. Torrents E. Ribonucleotide reductases: essential enzymes for bacterial life. Front Cell Infect
702 Microbiol. 2014; 4: 52.
- 703 63. Borovok I, Gorovitz B, Schreiber R, Aharonowitz Y, Cohen G. Coenzyme B12 controls
704 transcription of the *Streptomyces* class Ia ribonucleotide reductase *nrdABS* operon via a
705 riboswitch mechanism. J Bacteriol. 2006; 188(7): 2512–2520.
- 706 64. Boer JL, Mulrooney SB, Hausinger RP. Nickel-dependent metalloenzymes. Arch Biochem
707 Biophys. 2014; 0: 142–152.
- 708 65. Hattori M, Iwase N, Furuya N, Tanaka Y, Tsukazaki T, *et al.* Mg²⁺-dependent gating of
709 bacterial MgtE channel underlies Mg²⁺ homeostasis. EMBO J. 2009; 28(22): 3602–3612.
- 710 66. Moreno-Vivián C, Cabello P, Martínez-Luque M, Blasco R, Castillo F. Prokaryotic nitrate
711 reduction: molecular properties and functional distinction among bacterial nitrate
712 reductases. J Bacteriol. 1999; 181(21): 6573–6584.
- 713 67. Marcia M, Ermler U, Peng G, Michel H. A new structure-based classification of
714 sulfide:quinone oxidoreductases. Proteins 2010; 78: 1073–1083.

- 715 68. Gregersen LH, Bryant DA, Frigaard NU. Mechanisms and evolution of oxidative sulfur
716 metabolism in green sulfur bacteria. *Front Microbiol.* 2011; 2: 116.
- 717 69. Shuman KE, Hanson TE. A sulfide:quinone oxidoreductase from *Chlorobaculum tepidum*
718 displays unusual kinetic properties. *FEMS Microbiol Lett.* 2016; 363: fnw100.
- 719 70. Pruski AM, Fiala-Médioni A. Stimulatory effect of sulphide on thiotaurine synthesis in three
720 hydrothermal-vent species from the East Pacific Rise. *J Exp Biol.* 2003; 206: 2923–2930.
- 721 71. Rosenberg NK, Lee RW, Yancey PH. High contents of hypotaurine and thiotaurine in
722 hydrothermal-vent gastropods without thiotrophic endosymbionts. *J Exp Zool Pt A* 2006;
723 305(8): 655–662.
- 724 72. Brand GL, Horak RV, Le Bris N, Goffredi SK, Carney SL, *et al.* Hypotaurine and thiotaurine
725 as indicators of sulfide exposure in bivalves and vestimentiferans from hydrothermal vents
726 and cold seeps. *Mar Ecol.* 2007; 28(1): 208–218.
- 727 73. Dominy Jr JE, Simmons CR, Karplus PA, Gehring AM, Stipanuk MH. Identification and
728 characterization of bacterial cysteine dioxygenases: a new route of cysteine degradation for
729 eubacteria. *J Bacteriol.* 2006; 188(15): 5561–5569.
- 730

731 **Acknowledgements**

732 We thank the able captains and crews of the R/Vs *Atlantis*, *Western Flyer* and *Point Lobos* as
733 well as the pilots of the submersibles *Alvin*, *Tiburon* and *Ventana* for supporting the sample
734 collections. We further thank N. Pratt and A. Baylay for their contributions to library preparation
735 and high-throughput sequencing at the National Oceanography Centre Genomics Facility. This
736 work was supported by grants of the David and Lucile Packard Foundation (to MBARI), the UK
737 Natural Environment Research Council (grant number NE/N006496/1 to C.R.Y.), the United
738 States National Science Foundation (grant number OCE-1736932 to R.A.B.) and National
739 Capability funding to the National Oceanography Centre (grant number NE/R015953/1). M.P.'s
740 contribution was funded through the Alexander Graham Bell Canada Graduate Scholarship and
741 the Michael Smith Foreign Study Supplements granted by the Natural Sciences and Engineering
742 Research Council of Canada.

743

744 **Author Contributions**

745 C.B. and M.P. performed the majority of statistical analyses and co-wrote the paper. R.A.B.
746 contributed to data interpretation and co-wrote the manuscript. C.R.Y. designed the study,
747 contributed to data collection and analysis and co-wrote the manuscript.

748

749 **Competing Interests**

750 The authors declare no competing interests.

751

752 **Figure Legends**

753 **Figure 1** Bayesian phylogeny of the *16S* rRNA gene for vesicomylid symbionts (A) and
754 pangenomic comparison based on 3,208 gene clusters organized according to their distribution
755 across genomes. Each symbiont genome is represented as a circle layer, with *Ca.*
756 *Vesicomysocius* lineages shown in green and *Ca. Ruthia* lineages shown in red. Dark color
757 shades within layers denote presence of a gene cluster, whereas light shades denote absence.
758 Gene cluster groups representative of the core genome (grey), *Ca. Vesicomysocius*-specific
759 genome (green) and *Ca. Ruthia*-specific genome (red) are indicated. The top right dendrogram
760 shows phylogenomic relationships among symbiont genomes based on 739 single copy gene
761 clusters. Average nucleotide identities (80–100%) among genomes are presented below the
762 dendrogram based on a color gradient, where darker shades indicate higher similarities.

763

764 **Figure 2** (A) Core genome of vesicomylid symbiont based on categorization into Clusters of
765 Orthologous Groups (COGs). (B) Functional categorization of gene clusters specific to *Ca.*
766 *Vesicomysocius* and *Ca. Ruthia*. Some gene clusters are functionally related to various
767 metabolic pathways and are therefore classified into multiple categories.

768

769 **Figure 3** Main differences in metabolic gene content between *Ca. Vesicomysocius* and *Ca.*
770 *Ruthia* and presence/absence of essential genes related to DNA repair, recombination and anti-
771 viral defense. A detailed description is given in the manuscript text.

772 **Tables**

773 **Table 1** General information about vesicomid symbiont genomes compared in this study.
774

Symbiont	Accession No.	Genome size (Mb)	# Contigs	N50 (Mb)	GC (%)	Coverage (X)	# CDS	# RNAs	Reference
<i>Ca. R. magnifica</i>	CP000488	1.16	1	1.16	34.03	14.00	976	39	Newton et al. (2007)
<i>Ca. R. pacifica</i>	CP060683	1.18	1	1.18	36.58	140.20	1,456	38	This study
<i>Ca. R. phaseoliformis</i>	JACRUR000000000	1.53	8	0.37	36.93	69.48	2,210	39	This study
<i>Ca. R. pliocardia</i>	CP060688	1.23	1	1.23	36.98	113.20	1,643	39	This study
<i>Ca. R. rectimargo</i>	CP060684	1.19	1	1.19	36.69	90.80	1,476	40	This study
<i>Ca. R. southwardae</i>	JACRUS000000000	1.59	39	0.06	36.86	89.56	2,035	39	This study
<i>Ca. V. diagonalis</i>	CP060680	1.02	1	1.02	31.10	110.30	1,005	39	This study
<i>Ca. V. extenta</i>	CP060685	1.02	1	1.02	31.10	137.00	995	39	This study
<i>Ca. V. gigas 1</i>	CP060681	1.03	1	1.03	31.37	49.20	1,008	39	This study
<i>Ca. V. gigas 2</i>	CP060682	1.03	1	1.03	31.38	153.10	979	39	This study
<i>Ca. V. okutanii</i>	AP009247	1.02	1	1.02	31.59	9.00	937	38	Kuwahara et al. (2007)
<i>Ca. V. soyoae 1</i>	CP060687	1.02	1	1.02	31.63	89.40	992	39	This study
<i>Ca. V. soyoae 2</i>	CP060686	1.02	1	1.02	31.63	109.90	983	39	This study

775
776
777 **Table 2** Sampling information for vesicomid hosts.
778

Host species	Symbiont	Locality	Latitude	Longitude	Depth (m)	Habitat	Dive # ^a	Year
<i>Abyssogena phaseoliformis</i>	<i>Ca. R. phaseoliformis</i>	Aleutian Trench	54.3050	-157.2133	3550	Seep	- ^b	1996

<i>Abyssogena southwardae</i>	<i>Ca. R. southwardae</i>	Logatchev	14.7532	-44.9805	3038	Vent	A: 3133	1997
<i>Archivesica diagonalis</i>	<i>Ca. V. diagonalis</i>	Monterey Canyon	36.2274	-122.8796	3456	Seep	T: 488	2002
<i>Archivesica gigas</i> (1)	<i>Ca. V. gigas</i> 1	East Gorda Escarpment	40.3580	-125.0210	2094	Vent	T: 351	2001
<i>Archivesica gigas</i> (2)	<i>Ca. V. gigas</i> 2	Guaymas Transform Fault	27.3400	-111.2700	1754	Seep	T: 548	2003
<i>Calypptogena magnifica</i>	<i>Ca. R. magnifica</i>	East Pacific Rise	9.8480	-104.2935	2507	Vent	A: 3951	2004
<i>Calypptogena pacifica</i>	<i>Ca. R. pacifica</i>	Monterey Canyon	36.7739	-122.0488	650	Seep	V: 2555	2004
<i>Calypptogena rectimargo</i>	<i>Ca. R. rectimargo</i>	Monterey Canyon	36.6816	-122.1197	1540	Seep	V: 2338	2003
<i>Phreagena extenta</i>	<i>Ca. V. extenta</i>	Monterey Canyon	36.6088	-122.4366	2889	Seep	T: 406	2002
<i>Phreagena okutanii</i>	<i>Ca. V. okutanii</i>	Sagami Bay	37.9500	139.2000	1157	Seep	HD: 305	2004
<i>Phreagena soyoae</i> (1)	<i>Ca. V. soyoae</i> 1	Oregon Subduction Zone	44.6755	-125.1182	765	Seep	A: 2796	1994
<i>Phreagena soyoae</i> (2)	<i>Ca. V. soyoae</i> 2	Monterey Canyon	36.7762	-122.0842	985	Seep	V: 2059	2001
<i>Pliocardia</i> sp.	<i>Ca. R. pliocardia</i>	Blake Spur	32.4948	-76.1847	2155	Seep	A: 3710	2001

779 ^aSubmersibles: A = *Alvin*, HD = *Hyper Dolphin*, T = *Tiburón*, V = *Ventana*

780 ^bSampled with TV grab

781

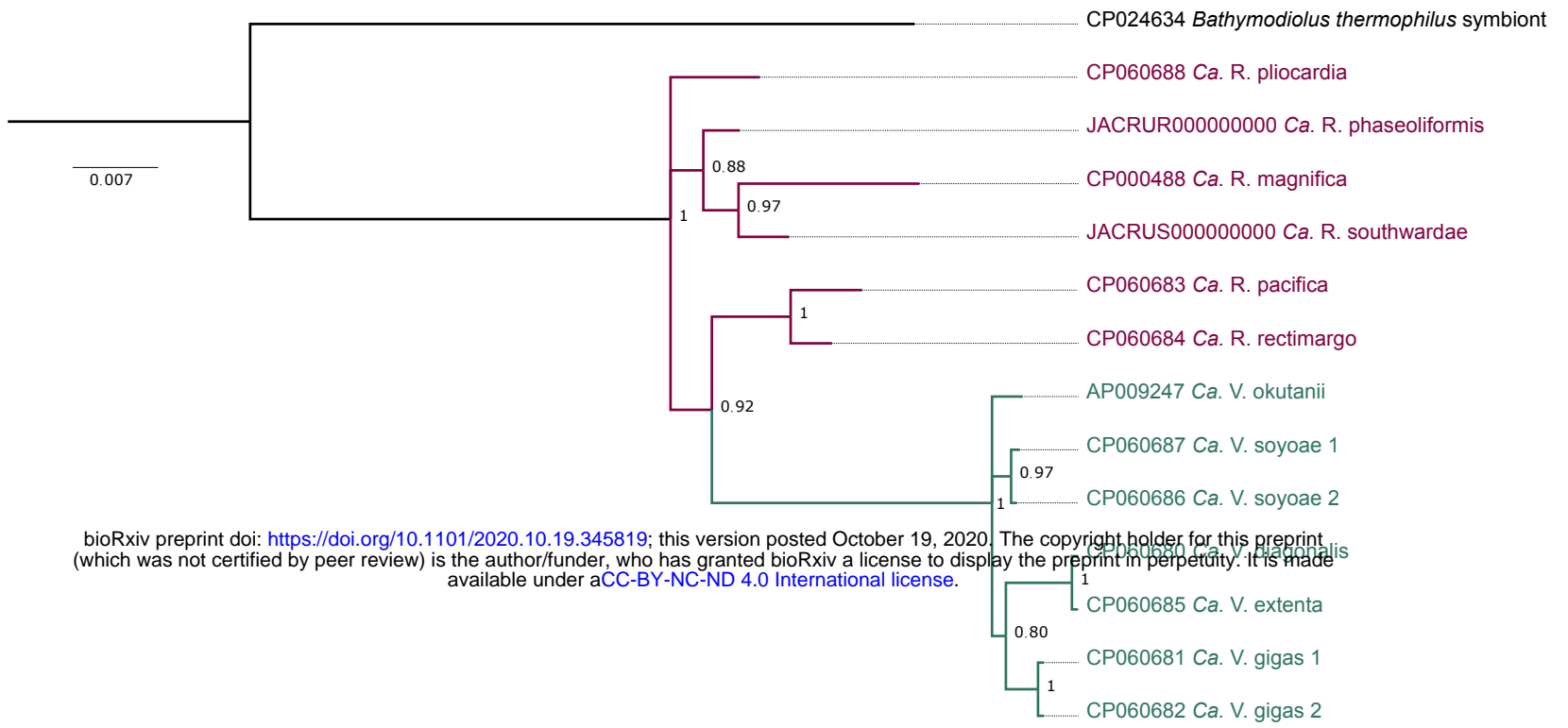
782 **Table 3** Sites under pervasive or episodic positive selection in 10 candidate genes based on FUBAR and MEME analyses. α = synonymous substitution rate at a
 783 site; $\beta+$ = non-synonymous substitution rate at a site for the positive/neutral evolution component; Pr = posterior probability (a value ≥ 0.9 indicates strong
 784 evidence for positive selection); $q+$ = very approximate proportion of branches evolving under positive selection; LRT = likelihood ratio test statistic for episodic
 785 diversification; p = p-value for episodic diversification (a value ≤ 0.1 indicates positive selection).
 786

Site	α	FUBAR			MEME				
		$\beta+$	Pr	α	$\beta+$	$q+$	LRT	p	
<i>cdo</i>	65	1.4130	15.5050	0.9044	0.0000	94.6310	0.1380	4.8230	0.0413
	156	–	–	–	0.0000	1.2290	1.0000	3.3470	0.0890
<i>hupE</i>	39	2.7030	15.5090	0.9157	0.0000	33.0330	0.4180	5.2300	0.0335

	49	–	–	–	1.2160	261.8800	0.1010	5.7280	0.0259
	86	–	–	–	0.0000	6.1150	0.2910	4.5500	0.0476
	134	–	–	–	0.0000	4.7840	0.4770	5.1880	0.0342
	333	0.9250	8.8230	0.9314	0.0000	3.8540	1.0000	3.2000	0.0961
	373	–	–	–	1.1930	2433.1130	0.0970	4.3520	0.0527
<i>metE</i>	49	–	–	–	0.0000	126.9650	0.0970	5.3060	0.0322
	218	0.8680	8.8950	0.9377	0.0000	2.6500	1.0000	3.9300	0.0656
	234	–	–	–	0.7460	15.5340	0.2040	3.6460	0.0761
<i>metH</i>	123	–	–	–	0.0000	53.7870	0.0980	3.1960	0.0963
	129	–	–	–	0.0000	19.1500	0.3300	3.3170	0.0904
	615	–	–	–	0.6390	79.7860	0.0950	3.9620	0.0645
	621	–	–	–	0.4440	25.2060	0.1050	5.9500	0.0231
	654	–	–	–	0.0000	8.6840	0.1270	3.2490	0.0937
	749	–	–	–	0.4410	8.5390	0.3660	3.6720	0.0751
	902	–	–	–	0.0000	1.4390	0.3070	3.4000	0.0865
	953	–	–	–	0.3650	10.8580	0.1290	4.6050	0.0462
<i>narG</i>	138	–	–	–	0.0000	7.5290	0.2350	3.8440	0.0686
	451	4.2920	39.0210	0.9409	0.0000	21.5910	1.0000	2.4350	0.1441 [†]
<i>narH</i>	54	–	–	–	0.0000	11.1380	0.2230	3.9820	0.0639
<i>narI</i>	–	–	–	–	–	–	–	–	–
<i>narJ</i>	211	–	–	–	0.0000	7.3140	0.2790	3.5150	0.0815
	216	–	–	–	0.0000	3.9790	0.3420	3.5750	0.0790

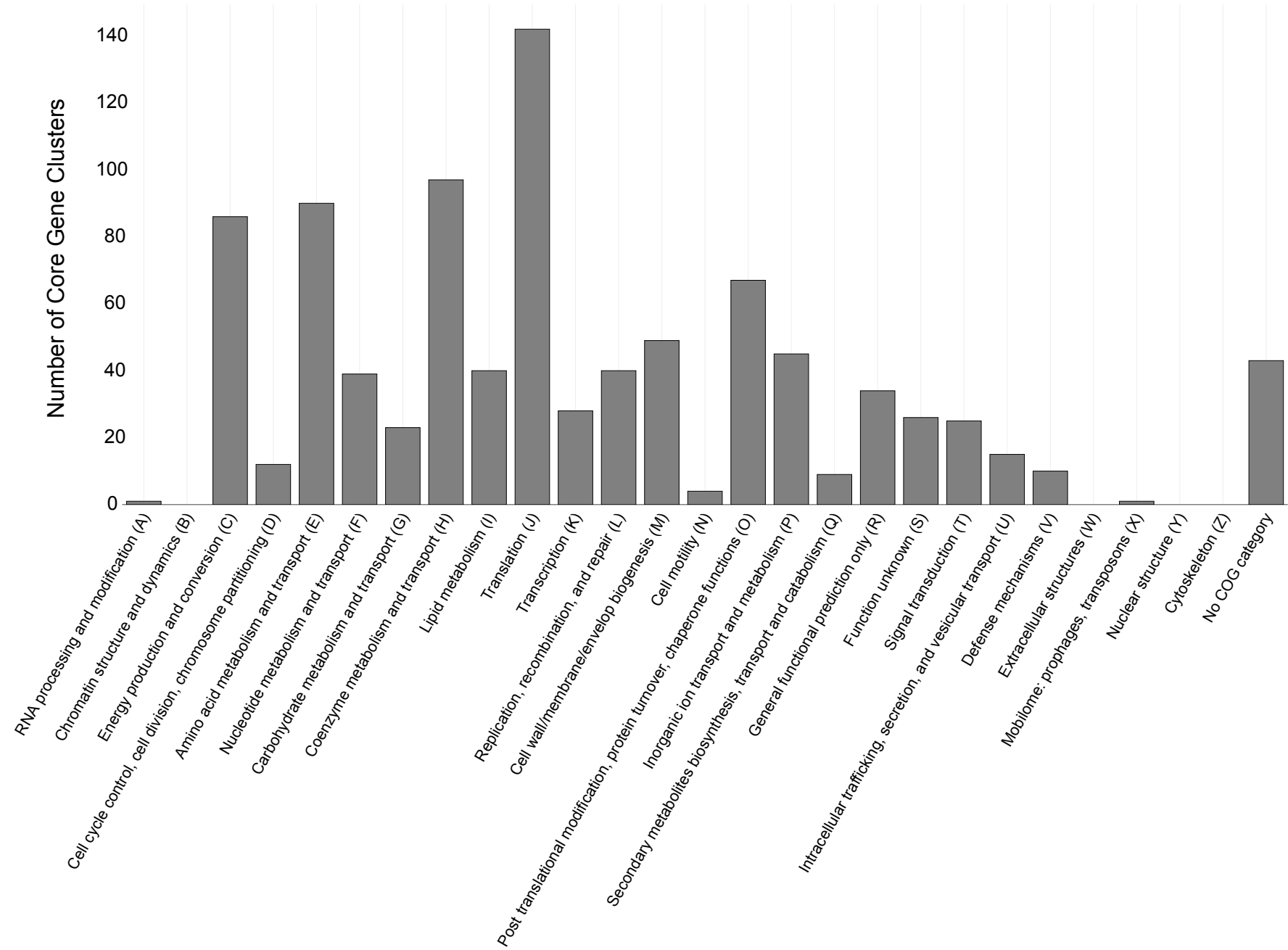
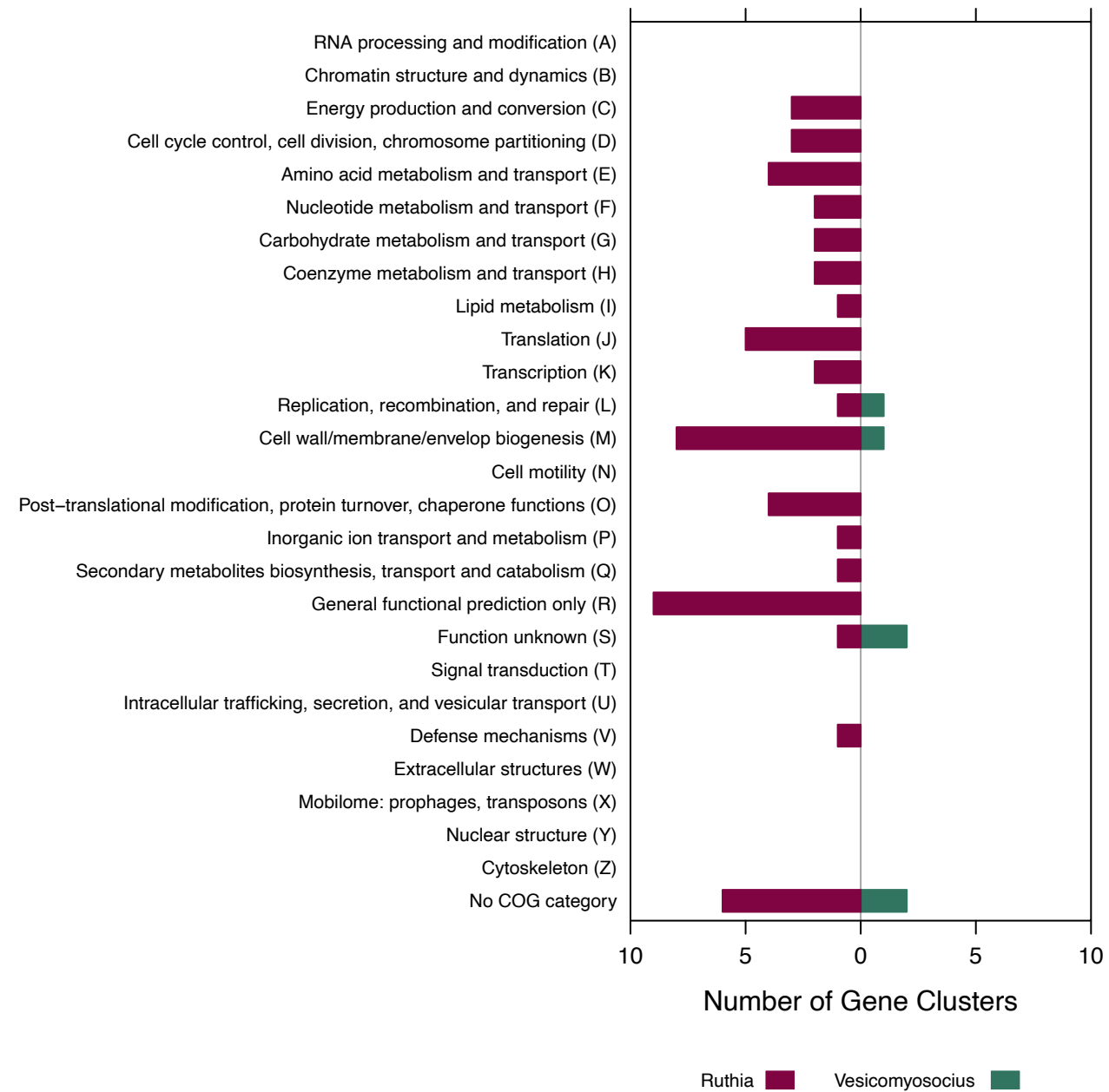
<i>nasA</i>	70	0.5960	12.9980	0.9580	0.0000	2.8050	1.0000	3.6770	0.0749
	79	–	–	–	0.0000	23.6900	0.1400	4.5030	0.0487
	451	1.4360	13.6900	0.9362	0.0000	3.6150	0.9990	2.1190	0.1707 [†]
<i>sqrI</i>	4	0.6890	6.2540	0.9475	0.0000	1.5310	0.9970	2.9470	0.1098 [†]
	168	–	–	–	3.2830	50.0800	0.0520	3.9720	0.0642
	366	–	–	–	0.6110	42.3580	0.1110	5.5300	0.0287
	428	–	–	–	0.0000	10000.0000	0.0830	3.7640	0.0715

787 [†]Test was not significant

A

bioRxiv preprint doi: <https://doi.org/10.1101/2020.10.19.345819>; this version posted October 19, 2020. The copyright holder for this preprint (which was not certified by peer review) is the author/funder, who has granted bioRxiv a license to display the preprint in perpetuity. It is made available under aCC-BY-NC-ND 4.0 International license.

B

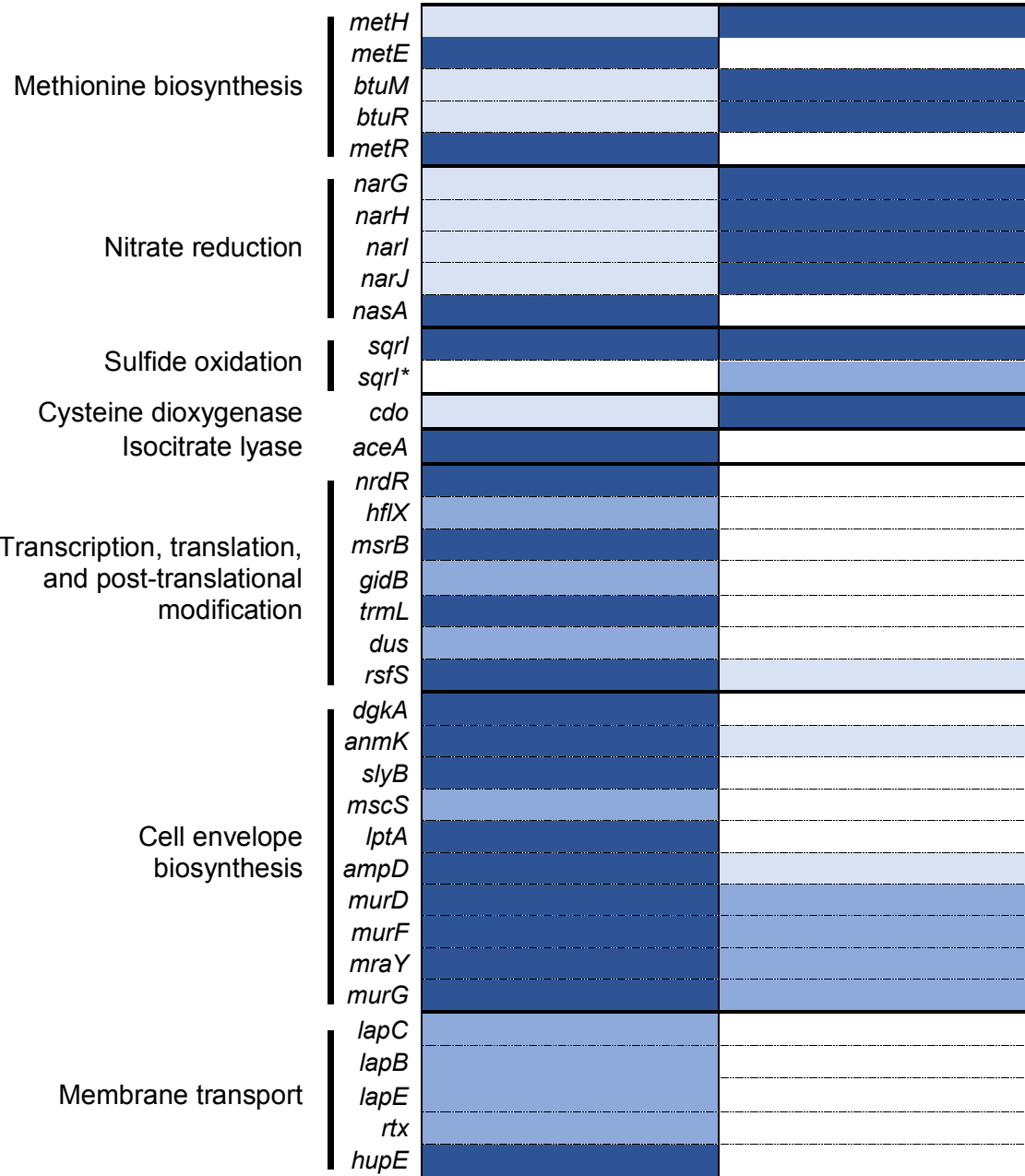
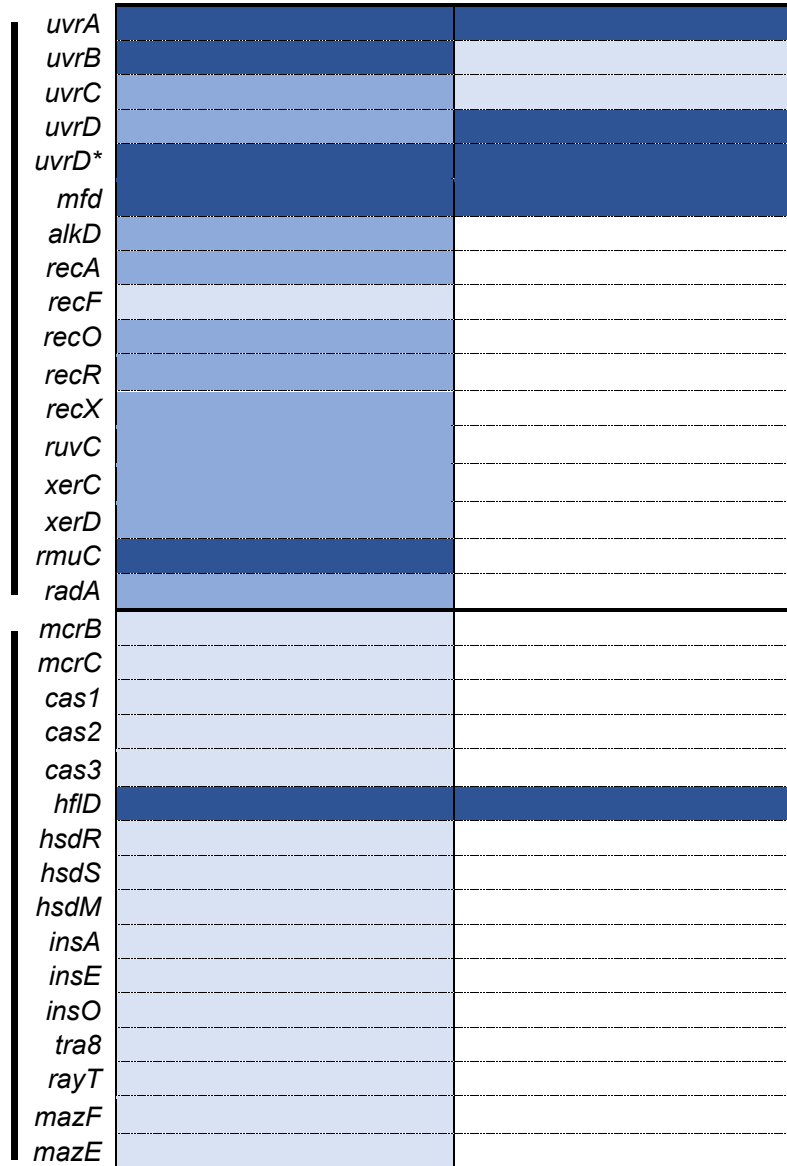
A**B**

Ca. Ruthia

Ca. Vesicomysocius

Ca. Ruthia

Ca. Vesicomysocius

DNA repair and
recombination

* indicates paralogous gene



absent in all lineages



present in a few lineages or only remnants



present in most lineages



present in all lineages